



## H2020 Grant Agreement No. 730562 – RadioNet

<b>PROJECT TITLE:</b>	Advanced Radio Astronomy in Europe
<b>STARTING DATE</b>	01/01/2017
<b>DURATION:</b>	48 months
<b>CALL IDENTIFIER:</b>	H2020-INFRAIA-2016-1
<b>TOPIC:</b>	INFRAIA-01-2016-2017 Integrating Activities for Advanced Communities



### Deliverable 7.7

#### Verification of RINGS software on BRAND dataset

Due date of deliverable: 2020-06-30

Actual submission date: 2020-11-13

Lead beneficiary (Number): JOINT INSTITUTE FOR VERY LONG BASELINE  
INTERFEROMETRY AS AEUROPEAN RESEARCH  
INFRASTRUCTURE CONSORTIUM (JIV-ERIC) (5)

## Document information

Document name:	Verification of RINGS software on BRAND dataset
Type	Other
WP	WP7 – RINGS
Version date:	2020-11-13
Authors (Institutes)	Des Small (JIV-ERIC)

## Dissemination Level

Dissemination Level		
PU	Public	X
PP	Restricted to other programme participants (including the Commission Services)	
RE	Restricted to a group specified by the consortium (including the Commission Services)	
CO	Confidential, only for members of the consortium (including the Commission Services)	

## Index

1	Introduction.....	3
2	The CASA Software and Calibration Challenges.....	3
3	Single-Band Delays.....	5
4	Multiband Fringe Fitting .....	7
5	Conclusions .....	11

## ELUCIDATION:

Due to the Covid-19, the Art.51 applies to this deliverable. The original aim of this deliverable was a verification of the RINGS software on a dataset obtained from the BRAND receiver, developed in WP6 (BRAND EVN). The development of the BRAND receiver is delayed and will be finalised after the end of the RadioNet project. The present deliverable D7.7 is based on the data obtained from the VGOS system, which is comparable with the BRAND data. The verification of the RINGS software on VGOS data is thus the actual deliverable D7.7.

### 1 Introduction

The BRAND project<sup>1</sup> aims to build a prototype primary-focus receiver with a very wide frequency range from 1.5 GHz to 15.5 GHz, and to work towards equipping EVN stations with such receivers. The prototype was to be tested in summer of 2020, but partly due to the Covid-19 pandemic, this has not proved to be possible.

Since a single BRAND and VLBI observation requires at least two receivers, it was intended to use the BRAND receiver in combination with VGOS receivers at other sites for the preliminary test observations. VGOS receivers cover a frequency range from 2 to 14 GHz<sup>2</sup> and are therefore broadly compatible with BRAND, although they were developed primarily for geodetic observations and have a governance structure unconnected with the EVN. With the deployment of the BRAND receiver pushed back beyond the end date of the RINGS project, the decision was made to use VGOS receivers for testing the calibration software developed for this deliverable.

The members of the European-VGOS collaboration kindly provided data from their VGOS stations at WS (Wetzzel), YJ (Yebes), and OE (Onsala). In this observation the VGOS system uses 32 bands split into three subgroups of 8 bands across a frequency range from 3 GHz to 11 GHz. Each subband consists of 128 x 250 kHz channels, for a total bandwidth of 32 MHz. This frequency sampling of the data is a choice made for VGOS and doesn't reflect how we expect BRAND to be used, but it does offer an opportunity to see how our software handles the challenge of a sparsely sampled wide frequency band.

### 2 The CASA Software and Calibration Challenges

The CASA fringe-fitter has been extended during RINGS to handle both wide frequency bands and dispersive ionospheric delays; full details of this work are given in the report for deliverables D7.4 and D7.5.<sup>3</sup>

Figures 1 and 2 show two views of the uncalibrated phase for the baselines WE-YJ and WS-OE for a 30 second scan (scan 75 in the Measurement Set); Figure 1 shows the location of the bands across the range of frequency observed, but this makes it difficult to see the phase itself, and with both baselines plotted together, coloured by baseline; Figure 2 shows the sampled subbands plotted adjacent to each other and with the baselines split out, coloured by polarisation; in this case we see much more clearly the behaviour of the phase across the full range of the observed data, but we lose information about where the individual subbands are in the spectrum and even where the borders between subbands occur. Both plots are of a time average of phase for a single scan of VGOS data, and we show only the parallel hands of polarisation for each baseline.

---

<sup>1</sup> [http://publications.lib.chalmers.se/records/fulltext/253604/local\\_253604.pdf](http://publications.lib.chalmers.se/records/fulltext/253604/local_253604.pdf)

<sup>2</sup> <https://ivsc.gsfc.nasa.gov/technology/vgos-concept.html>

<sup>3</sup> [https://radiowiki.mpifr-bonn.mpg.de/lib/exe/fetch.php?media=jra:730562\\_radionet-d7.4-d7.5\\_200302.pdf](https://radiowiki.mpifr-bonn.mpg.de/lib/exe/fetch.php?media=jra:730562_radionet-d7.4-d7.5_200302.pdf)

In Figure 2 it can be clearly seen that the phase as a function of frequency is dominated by a gradient that looks roughly constant across the band, with wrapping at  $\pm 180^\circ$ , with jumps at the subband edges. This of course corresponds to a constant delay across the full band.

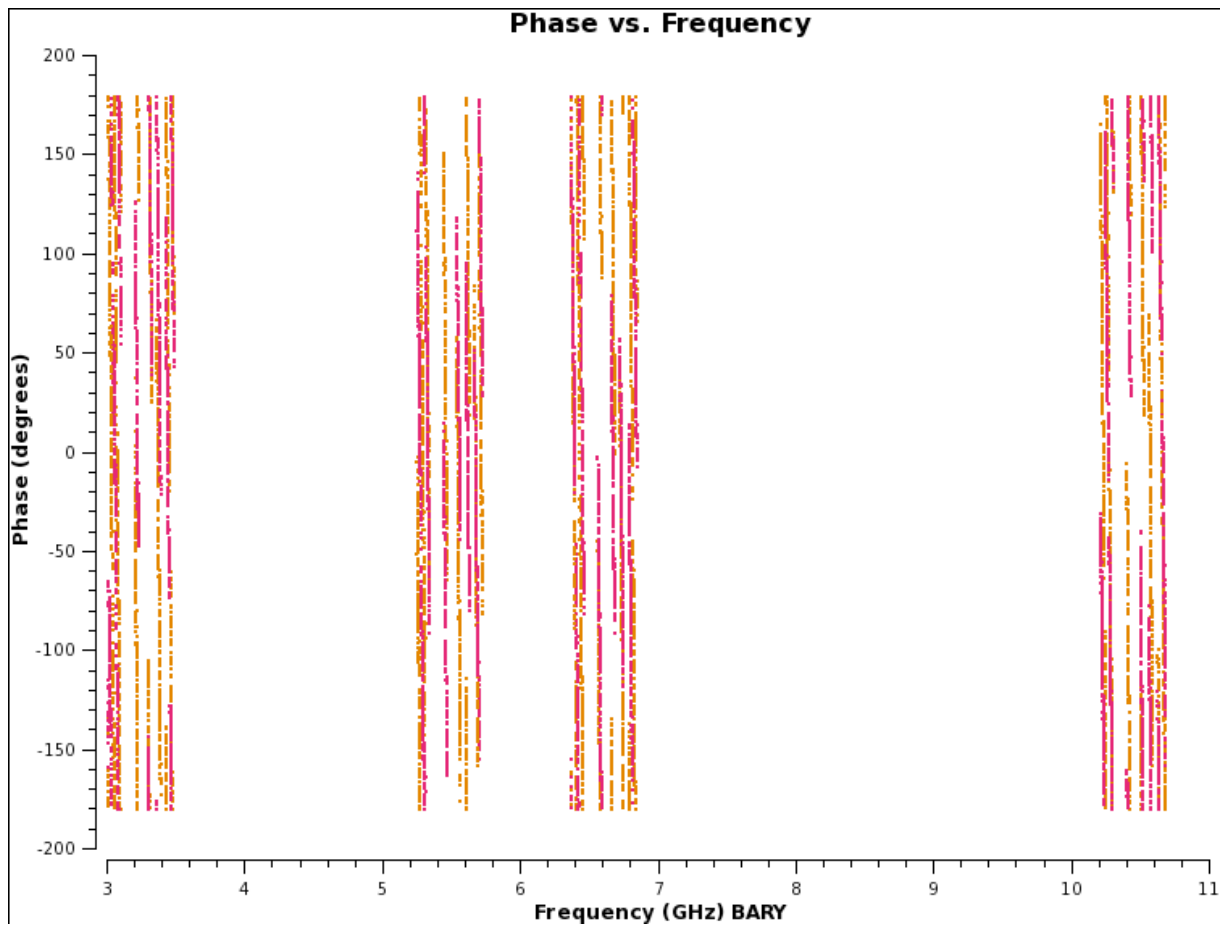
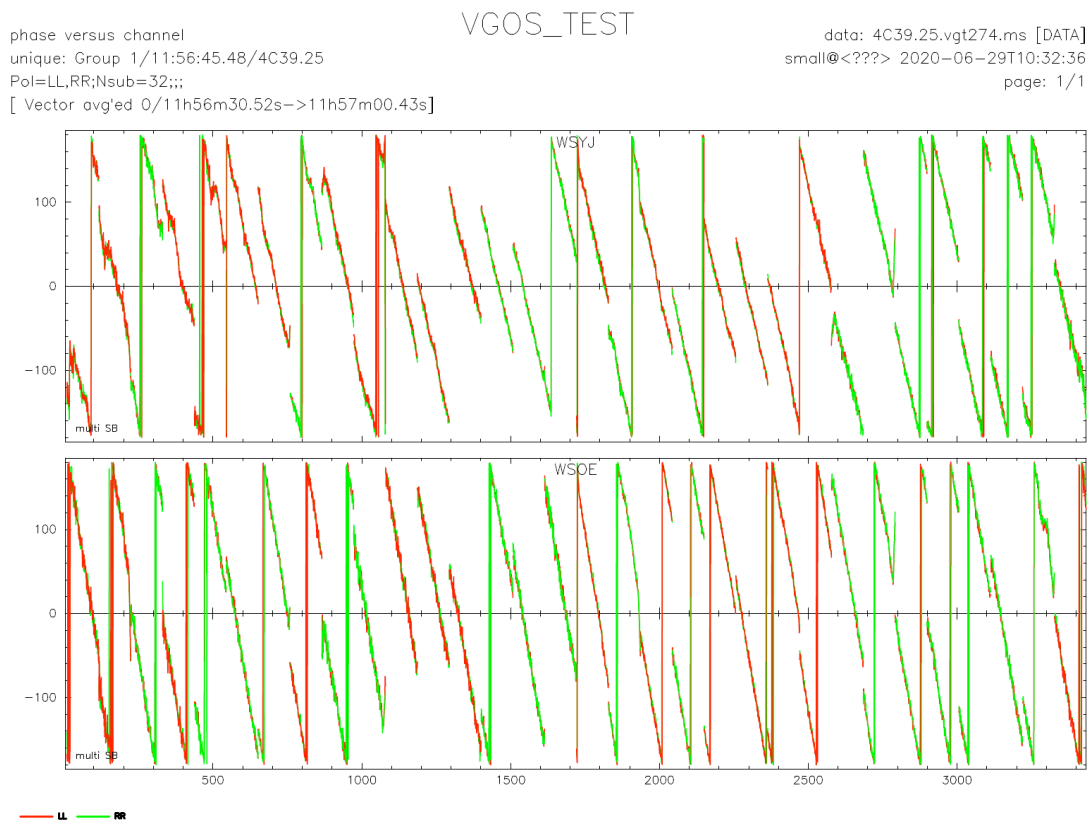


Figure 1: Phase as a function of frequency over the full bandwidth, before calibration.



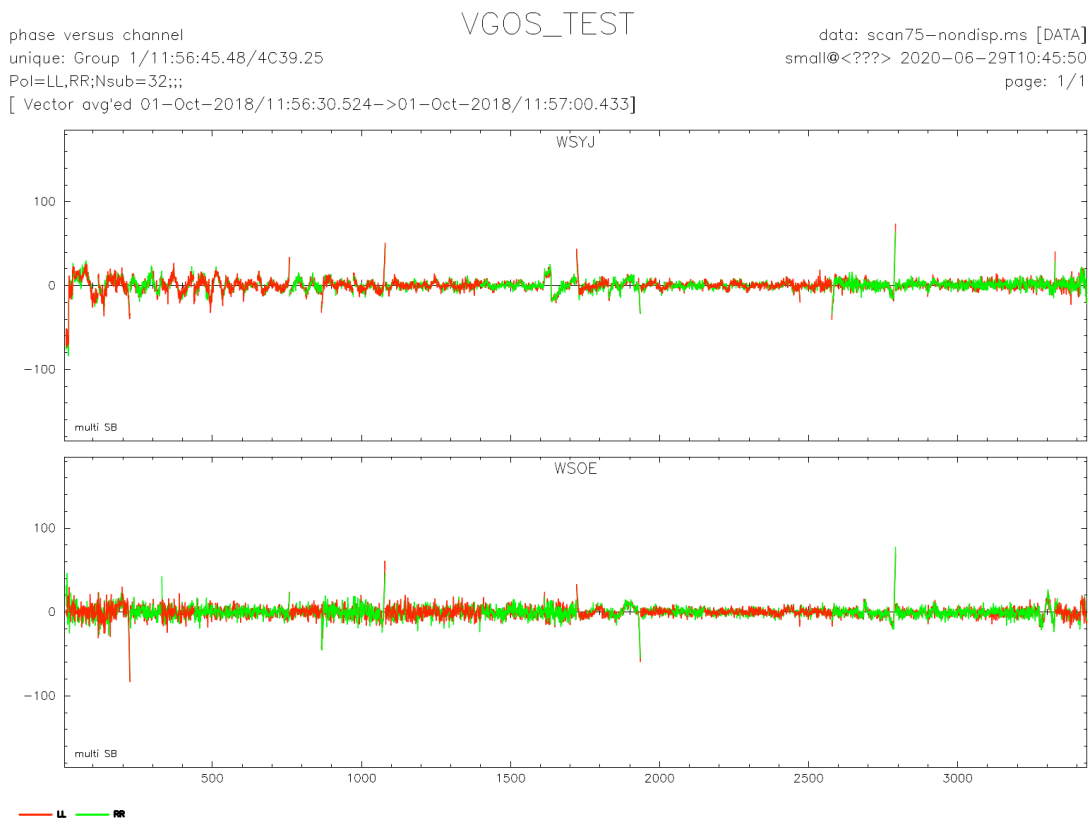
**Figure 2: Phase as a function of frequency over part of the bandwidth, before calibration,**

### 3 Single-Band Delays

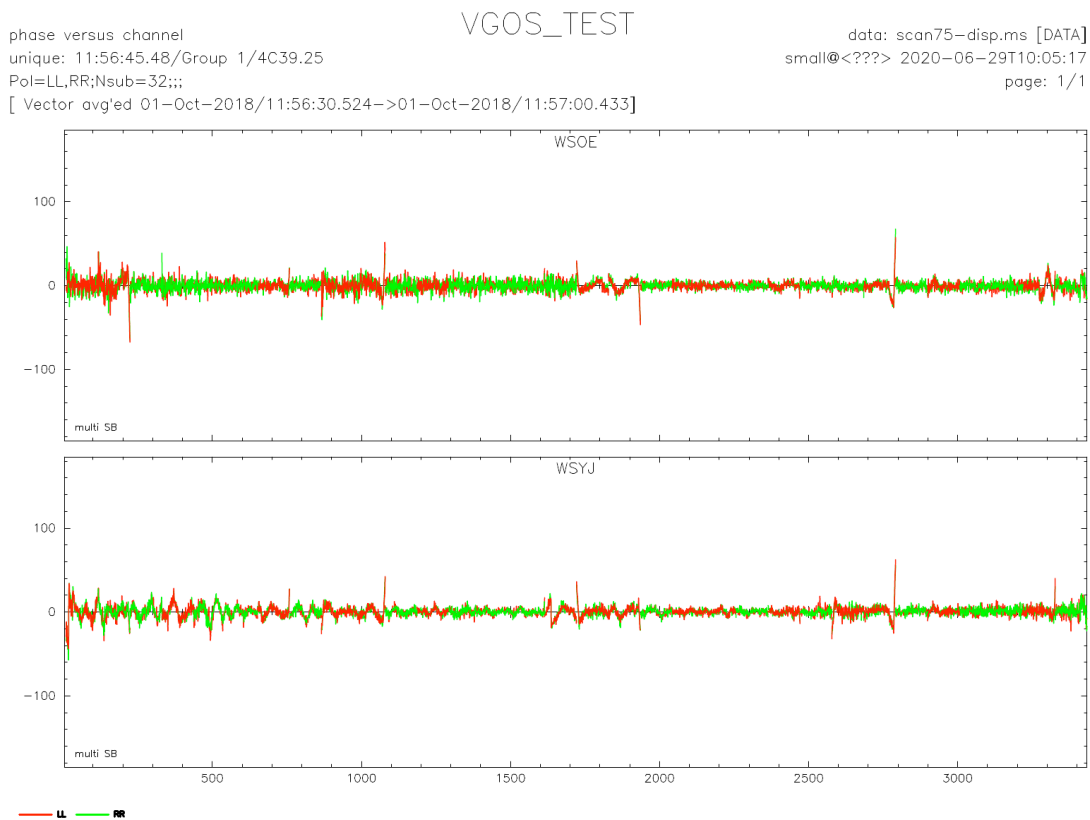
We note that all of the scans within the dataset are shorter when compared to typical VLBI observations. This is because VGOS is specialised for geodetic applications, where it is customary to observe as many sources as possible in an observation, and imaging is not traditionally a goal. However, it is also essential to get a high enough signal-to-noise ratio for accurate calibration, and the data used here is very well behaved in this respect.

Figure 3 shows the results of calculating and applying a fringe fit for each subband separately with only the delay and peculiar phase terms included in the calibration. This form of calibration is often used in VLBI as a “manual phase calibration” step that aligns the phases for the different subbands; this calibration can be applied to the whole data set, but for this to work we have decided to exclude a delay rate from our calibration since the effects of a spurious extrapolation of that term in time could dominate the calibration.

Figure 4 shows the same calibration with the dispersive term included, but with the delay-rate term still excluded. The baselines are in a different order, but it is visible that the calibrated data is slightly better at low frequencies with the dispersive term included.



**Figure 3: Phase as a function of frequency for scan 75, with non-dispersive fringe fitting.**



**Figure 4: Phase as a function of frequency for scan 75, with dispersive fringe fitting.**

## 4 Multiband Fringe Fitting

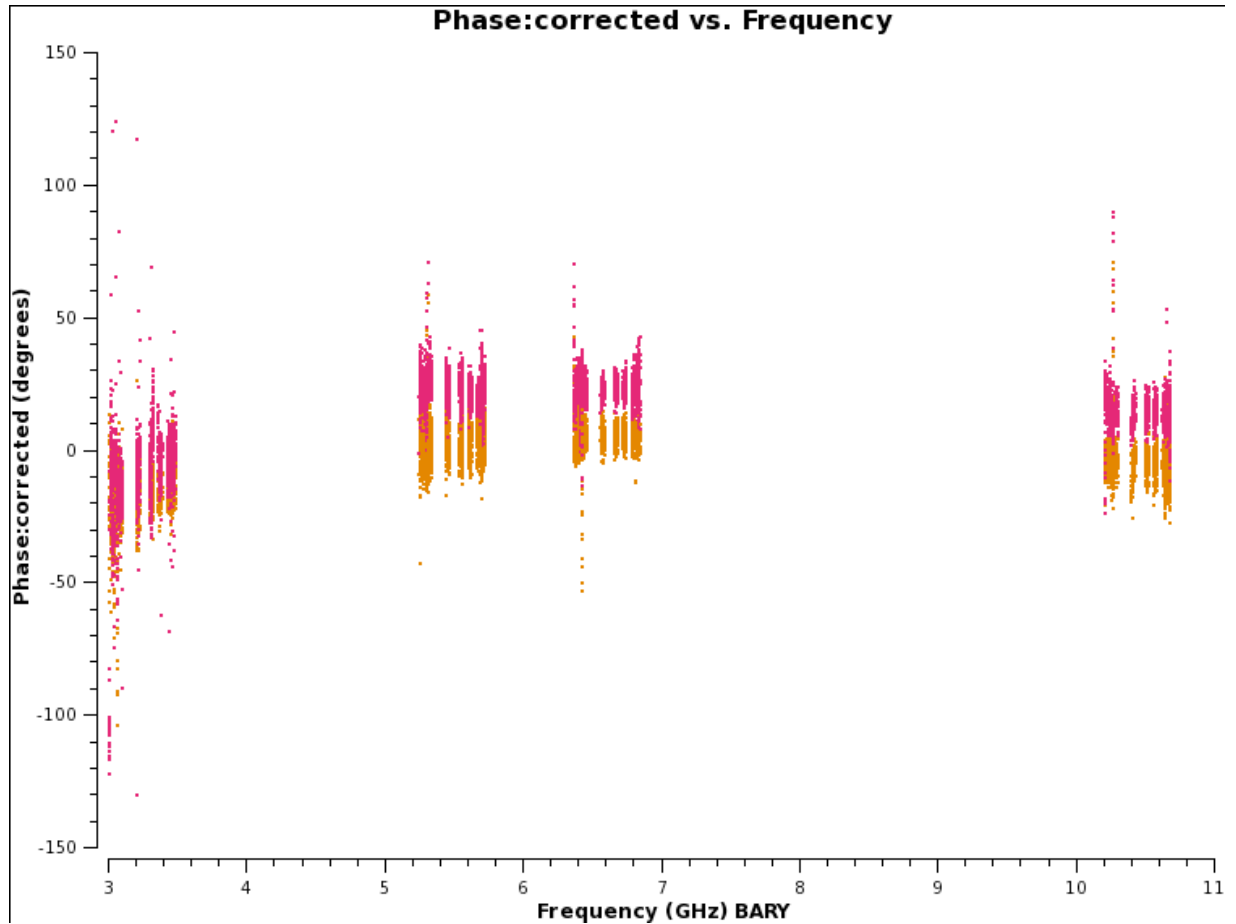
Once the single-band manual phase calibration has been derived and applied to the full dataset, the typical VLBI workflow is to do further calibration of the data on all of the subbands together using a single calibration model; the purpose of the manual phase calibration is precisely to make this possible. In this section we investigate whether this methodology is applicable to the very wide frequency ranges of VGOS (and implicitly BRAND) data.

Figure 5 shows the result of applying the non-dispersive manual phase calibration that is derived from scan 75 to a subsequent scan (scan 95) on the same source. We show here the data across the full sparsely sampled spectrum, as in Figure 1, since the eye is guided in this setting to see the residual curvature across the full frequency width. Since the dispersive delay due to the ionosphere is itself inversely proportional to the square of frequency, the resulting phase difference is proportional to the inverse of frequency, and when the linear part of that is removed by fitting a delay, the residual forms a curve around zero.

Finally, we show these results again with the subbands concatenated. Figure 7 shows the non-dispersive results, and Figure 8 the dispersive equivalent.

It is clear that the dispersive results are flatter across the full range of subbands, but it is noticeable that the individual subbands show signs of dispersive effects. This effect is presumably the result of an interplay between the dispersive correction at the single-band level and that of the multiband correction; if the size of the dispersive effect changes between the two scans, the single band correction applied to the new scan will leave precisely these sort of curves in the corrected data, and the multiband delay – which sees the data only after this correction has been applied – cannot compensate for it when solving for the overall dispersive effect.

In both the non-dispersive and dispersive cases we have used the CASA code developed for dispersive delays, with that option simply switched off when not required. The code proved more than capable of handling this bandwidth comfortably; the very wideband mode is currently being developed with application to the ongoing work of the EHT consortium, where the bandwidths are even larger and – crucially – not evenly aligned.



**Figure 5: Non-dispersive multiband fringe fit.**

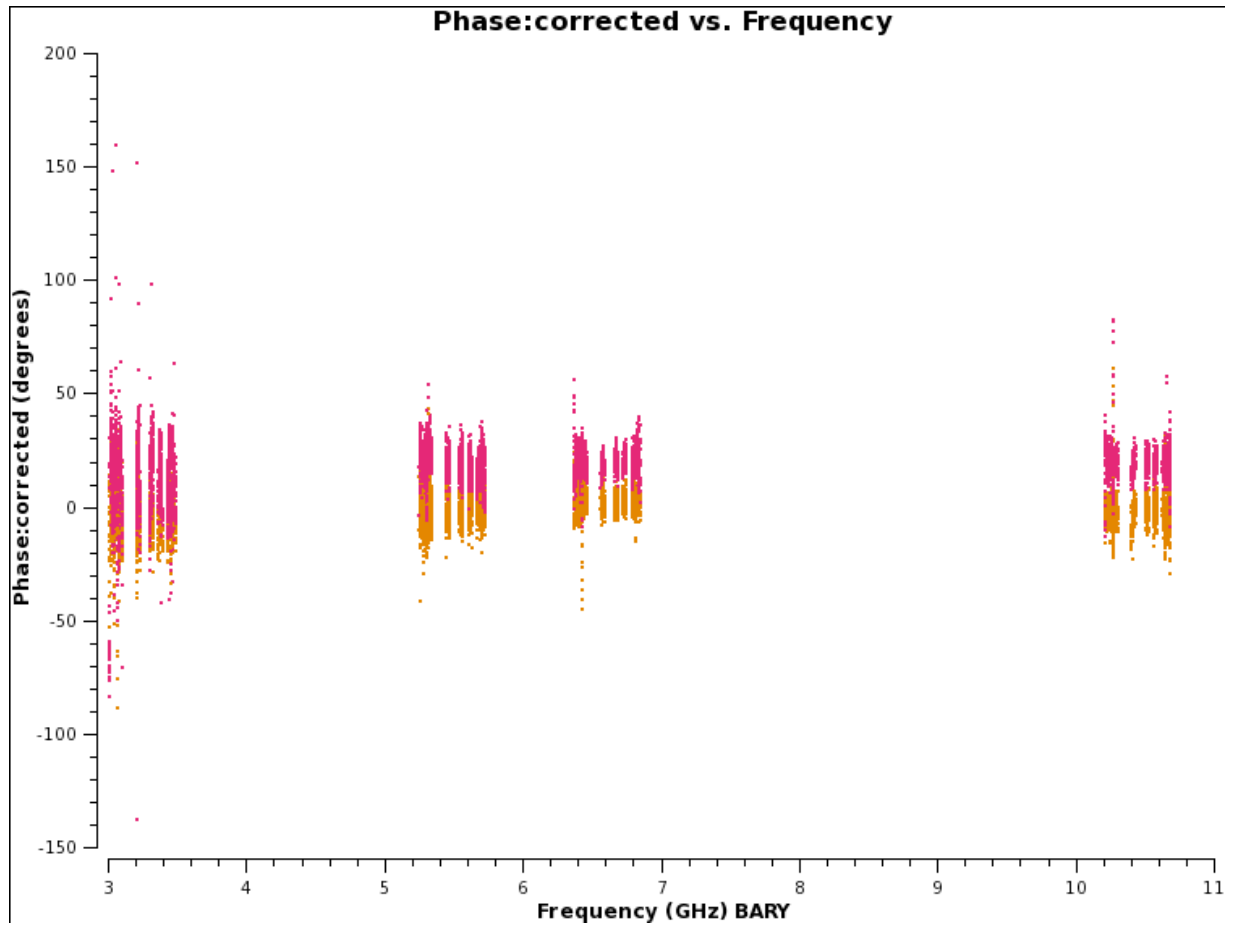
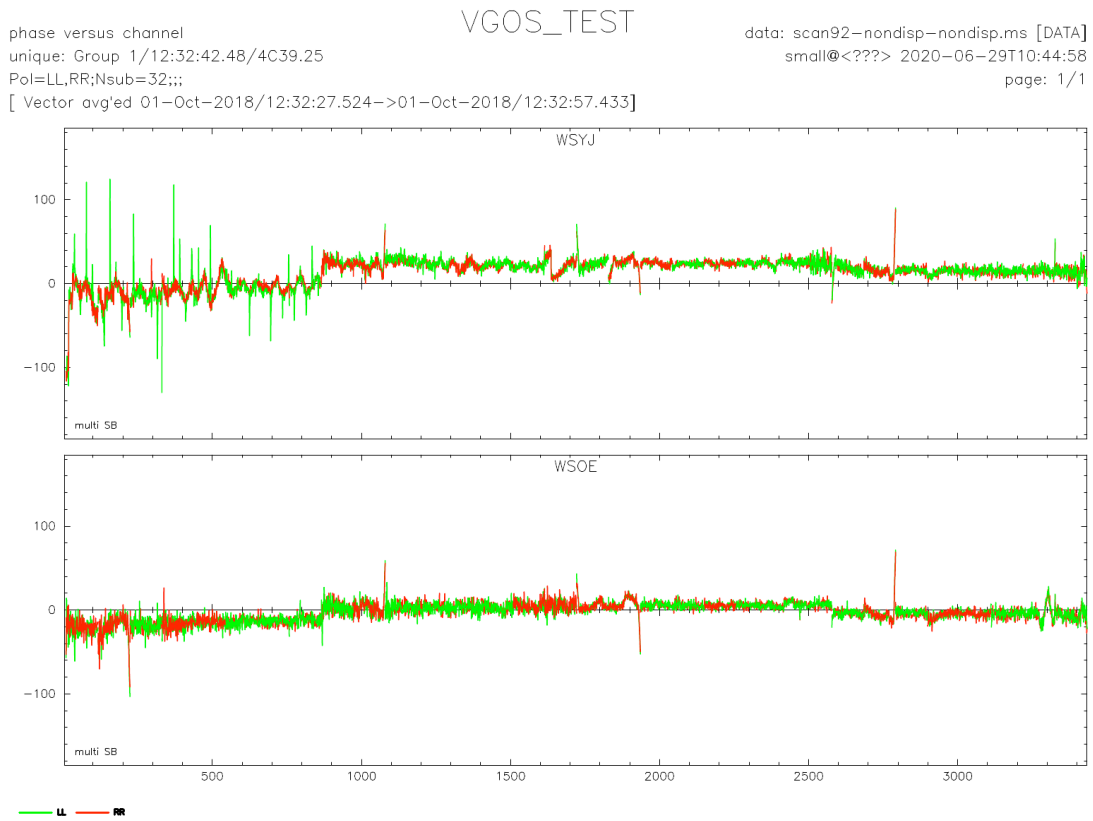
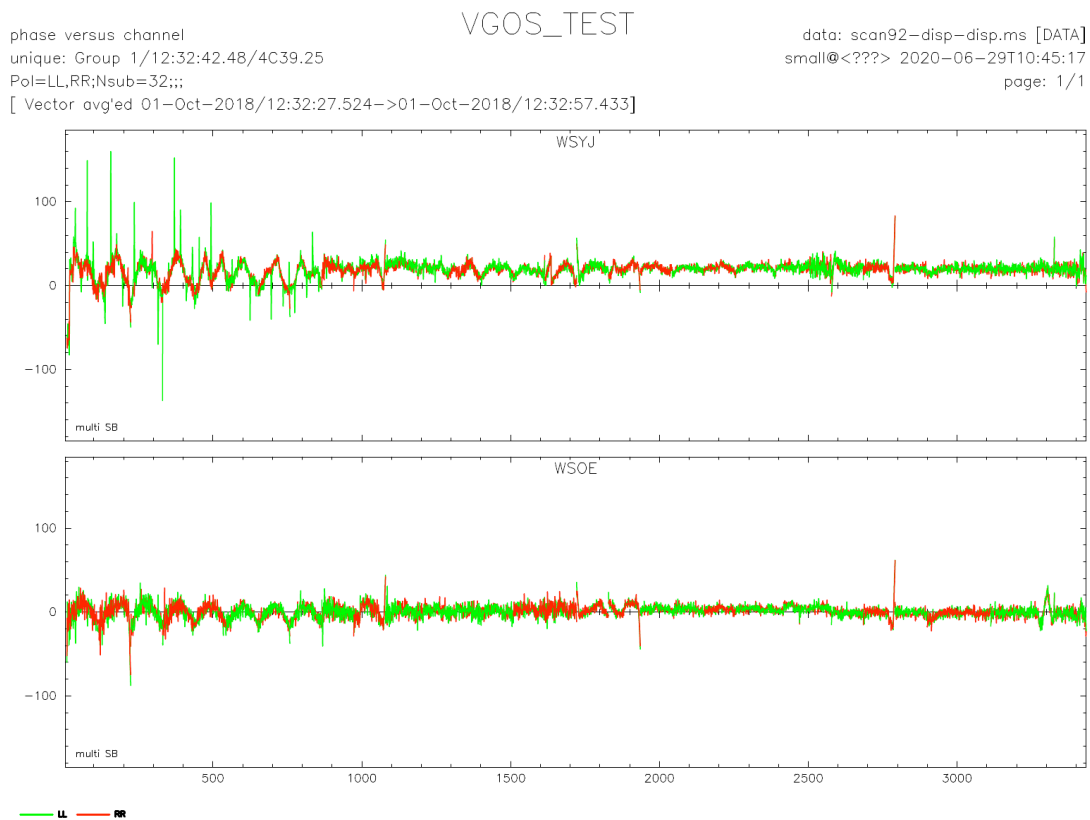


Figure 6: Dispersive multiband fringe fit.



**Figure 7: Non-dispersive multiband fringe fit.**



**Figure 8: Dispersive multiband fringe fit.**

## 5 Conclusions

We have demonstrated that the CASA fringe fitting software developed during RINGS can process VLBI data for an instrument with a frequency ratio of 10:1, although we have had to use VGOS data in place of BRAND data for the practical work. The fringe fitter can remove the dispersive effects due to the ionosphere that become noticeable in this regime, in addition to the usual delay and delay rate effects that are well-established in fringe-fitting. We do note, however, that the interaction of dispersive effects at the manual phase calibration stage and the subsequent multiband calibration stage has some modest residual effects that our methods do not yet account for.

© Copyright 2020 RadioNet

This document has been produced within the scope of the RadioNet Project.  
 The utilization and release of this document is subject to the conditions of the contract within the Horizon2020 programme, contract no. 730562